Available online at www.sciencedirect.com

SCIENCE DIRECT®

Materials Letters 60 (2006) 1484 – 1487

materials letters

www.elsevier.com/locate/matlet

Hydrothermal synthesis of hydroxyapatite nanopowders using cationic surfactant as a template

Yingjun Wang, Shuhua Zhang *, Kun Wei, Naru Zhao, Jingdi Chen, Xudong Wang

Key Laboratory of Specially Functional Materials and Advanced Manufacturing Technology (South China University of Technology), Ministry of Education, Guangzhou, 510640, China

Received 31 May 2005; accepted 18 November 2005
Available online 6 December 2005

Abstract

Hydroxyapatite (HAp) nanoparticles with uniform morphologies and controllable size have been synthesized successfully by low-temperature hydrothermal method. The cationic surfactant CTAB as a template is used to regulate the nucleation and crystal growth. The synthesized powders were characterized using X-ray diffraction, Fourier transform infrared spectrograph and transmission electron microscopy. The results indicate that the obtained particles are uniform rod-like monocrystals. Compared with the reaction time, the temperature of reaction is more significant variable in altering the HAp morphology and size. Furthermore, the behavior mechanism of CTAB is discussed.

Keywords: Hydrothermal synthesis; Hydroxyapatite; Surfactant; Template

1. Introduction

Hydroxyapatite (denoted as HAp), with the chemical formula $Ca_{10}(PO_4)_6(OH)_2$, has been extensively studied and applied in a variety of fields, due to its similarity with the mineral constituents of human bones and teeth [1–3]. Synthetic HAp has excellent biocompatibility and bioactivity, so it is used in reconstruction of damaged bone or tooth zones [4]. HAp also finds applications in others fields of industrial or technological interest as catalyst in chromatography or gas sensor [5], water purification, fertilizers production and drug carrier [6]. For load-bearing orthopedic and dental applications, densified HAps are largely needed. Unfortunately, due to its low mechanical reliability, especially in a wet environment [7], HAp bioceramics cannot be used for heavy load-bearing applications. Properties of HAp, including bioactivity, biocompatibility, solubility, sinterability, castability, fracture toughness and absorption can be tailored over wide ranges by controlling the particle composition, size and morphology [3,8–10]. For these reasons, it is of great importance to develop HAp synthesis methods focused on the precise control of particle size, morphology, and chemical composition.

Hap can be synthesized by many chemical-processing routes including solid-state reaction, co-precipitation, sol–gel synthesis, pyrolysis of aerosols, microemulsion and hydrothermal reaction [11]. These methods, however, mostly prepare irregular forms of powder. The conventional hydrothermal method has proved to be a convenient way to prepare materials, including salts, metal oxides, etc., but the control on morphology is also poor [12]. Bone itself is a composite consisting of HAp nanorods embedded in the collagen matrix [13]. Hence, HAp nanorods are desirable when biocompatibility is considered. The nucleation and crystal growth process mediated by macromolecule control and cell organization would finally result in uniform products [13]. The molecule-template addition has exerted significant control on the crystal morphology, which has been discussed by many review articles [14–18]. In the presence of extraneous additives, the role of the crystal surface is more analogous to the conventional view of host–guest systems. Organized organic surfaces can control the nucleation of inorganic materials by geometric, electrostatic and stereochemical complementarities between the incipient nuclei and the functionalized substrates [19–23].

* Corresponding author.
E-mail address: zhangshuhua2004@eyou.com (S. Zhang).

0167-577X/$ - see front matter © 2005 Elsevier B.V. All rights reserved.
doi:10.1016/j.matlet.2005.11.053

Table 1
The reaction conditions for the different cases

Experiment	H1	H2	H3	H4	H5	H6	H7
Temperature (°C)	120	120	120	120	60	90	150
Time (h)	12	16	20	24	20	20	20

In this paper, HAp nanoparticles with uniform morphologies and controllable size have been synthesized by hydrothermal method. The cationic surfactant CTAB as template is used as regulator of nucleation and crystal growth. The influences of the treatment temperature and the reaction time on crystal size and morphology have been investigated. The behavior mechanism of CTAB is also discussed.

2. Experimental

2.1. Materials and methods

The starting materials used in this work included calcium chloride ($CaCl_2$), dipotassium hydrogen phosphate ($K_2HPO_4{\cdot}3H_2O$), potassium hydroxide(KOH), cetyltrimethylammonium bromide (CTAB) and deionized water ($\geq$18.2 MΩ). All chemicals were analytical grade and aqueous solutions were made dissolving them in deionized water. All sample preparation solutions had a Ca/P ratio equal to 1.67 (stoichiometric ratio of HA).

The general procedure was the following: 0.024 mol of $K_2HPO_4{\cdot}3H_2O$ and 0.024 mol of CTAB were dissolved completely in 100 ml of deionized water by heating the solution to 50 °C and the pH value was adjusted to 12 by adding KOH solution (1 M). The mixed solution was kept 2 h to ensure the cooperative interaction and self-assembly process was completed. At the same time, 60 ml of the solution of calcium chloride ($CaCl_2$) (0.04 mol) was prepared. Then the $CaCl_2$ solution was added slowly in the mixed solution of $K_2HPO_4{\cdot}3H_2O$ and CTAB with continuous and gentle magnetic stirring. The final milky suspension was put in a teflon vessel, sealed tightly and heated in a oven at temperatures ranging between 60 and 150 °C for 12–24 h. The reaction conditions of different cases are shown in Table 1. The obtained precipitate was then filtered off and washed three times with ethanol and three times with deionized water to remove the residual CTAB and potassium ions and chloride ions. A gel-like paste was produced which was then dried at 70 °C for 24 h to yield white powders.

2.2. Characterization

The identification of the crystal phases of the obtained products was carried out by the X-ray diffraction (XRD) technique, using a Philips PW18v5/20 diffractometer with Cu-Kα incident radiation (40 kV, 30 Ma). The diffraction patterns were collected at room temperature over the 2θ range of 10–70°, with an acquisition time of 10.0 s at 0.01° step size.

Fourier transform infrared spectrograph (FTIR) was performed using a Perkin-Elmer Spectrum RX I spectrophotometer. Test samples were prepared by mixing ~2 mg of HAp powder and ~200 mg of spectroscopic-grade KBr (Merck) and pressing them to a disk at 15 MPa. Infrared spectra were recorded in the region 4000–400 cm^{-1}, with a resolution of 4.00 cm^{-1}.

The microstructural and morphological features of HA powders were investigated with a Philips EM430 ST transmission electron microscope (TEM) operated at 300 kV. Samples for TEM were prepared by air-drying a drop of a sonicated

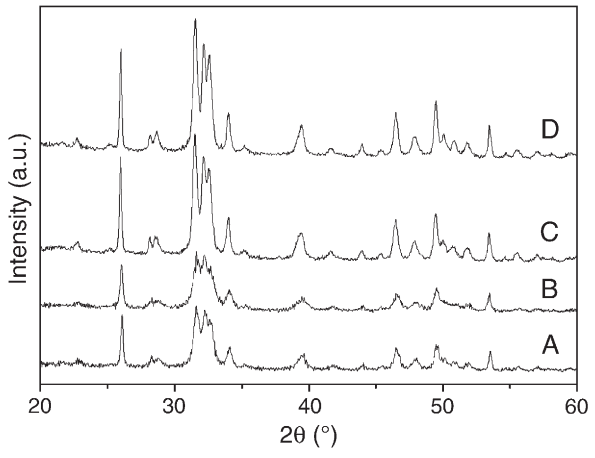

Fig. 1. The XRD diffraction patterns of the HAp powders obtain at 60 °C (A), 90 °C (B) and at 120 °C (C), 150 °C (D) for 20 h.

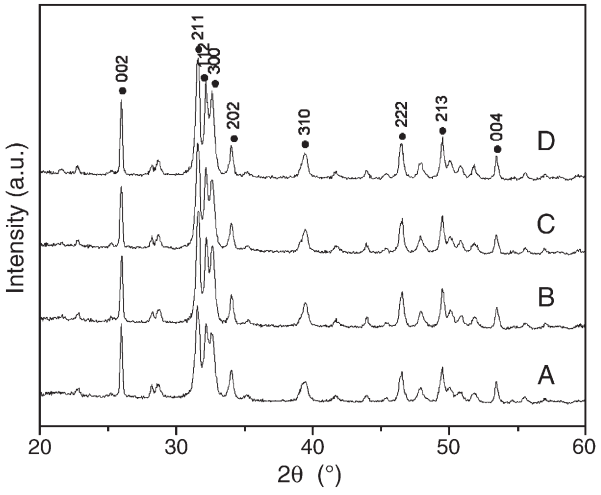

Fig. 2. The XRD patterns of the HAp powders obtained at 120 °C for 12 h (A), 16 h (B), 20 h (C) and 24 h (D).

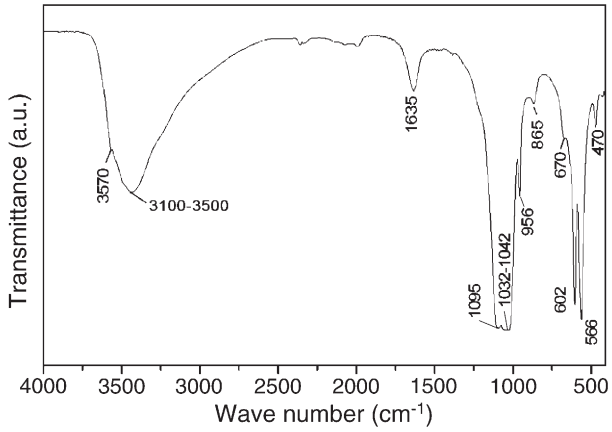

Fig. 3. The FTIR spectrum of the HAp powders obtained at 120 °C for 20 h.

ethanol suspension of particles onto a carbon-coated copper mesh.

3. Results and discussion

Fig. 1 shows the XRD patterns of HAp samples obtained at different synthesis temperatures. In general, the XRD patterns correspond to the characteristic peaks of HAp, but some differences may be observed. The XRD patterns of the HAp powders obtained at 60 and 90 °C (Fig. 1a and b) have wider and dispersed peaks, while those obtained at 120 and 150 °C (Fig. 1c and d) contain sharp peaks corresponding exactly to crystalline HAp with no additional peaks (File No. 73-0293, International Center for Diffraction Data, ICDD). So we may conclude that the HAp powders do not crystallize completely below 120 °C.

The XRD pattern of HAp powders synthesized at 120 °C for different hydrothermal reaction time are shown in Fig. 2. All four spectrums have many sharp HAp peaks and none corresponding to any impurity, suggesting that pure HA powders have been synthesized via hydrothermal processing at 120 °C with the reaction times of 12, 16, 20 and 24 h. Although the traces represent the characteristic XRD pattern for pure hydroxyapatite, the intensities of the 112 and 300 planes were changed due to the whisker orientation. This was also found in previous reports [24 25] about hydrothermal-synthesized HAp whiskers, which were apparently elongated along the c axis.

Fig. 3 shows the FTIR spectrums of the HAp powders obtained at 120 °C for 20 h. The 470 cm^{-1} band resulted from the v_2 phosphate mode [26]. The bands at 566, 602 cm^{-1} were derived from the v_4 bending vibrations of P–O mode and the 961 cm^{-1} band resulted from

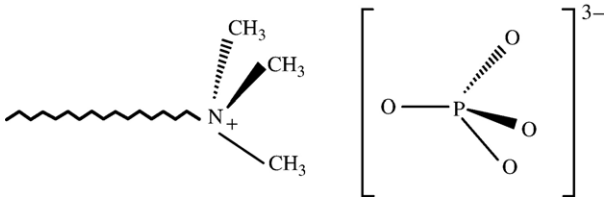

Fig. 5. A schematic drawing showing the complementarity between the surfactant cation and phosphate anion.

the v_1 symmetric P–O stretching vibration [27]. The two weak peaks at 865 and 670 cm^{-1} are attributed to carbonates [28], which reveals that a certain level of carbonate substitution has taken place in this sample, although this is not shown by the XRD phase analysis. The strong band at 1032–1042, 1095 cm^{-1} were also assigned to the P–O stretching vibration of PO_4^{3-} [29]. The above results revealed that the sample had high crystallinity. The broad band at 3100–3500 cm^{-1} corresponds to adsorbed water, while the weak peak at 3570 cm^{-1} corresponds to the stretching vibration of OH^{-1} ions in the HAp lattice [30]. No C–H stretching vibration bands were detected. The highly sensitive FTIR result indicated that no CTAB molecule was incorporated in the sample. This indicated that the quality of our sample was excellent and only a little carbonated HAP existed.

Fig. 4 shows the TEM photographs of HAp powders obtained at 120 °C for 20 h, 24 h and at 150 °C for 20 h. As can be seen, each of the three samples has uniform rod-like particles with different aspect ratios (i.e. length/diameter). From the TEM micrograph of HAp samples obtained at 120 °C for 20 h (Fig. 4A), the aspect ratio is about 3, with the crystal diameter and length equal to about 20 h and 60 nm, respectively. And at 120 °C for 24 h (Fig. 4B), HAp powder samples are much thinner and longer, with an aspect ratio about 5 and a typical diameter and length of about 15 nm and 75 nm, respectively. But for HAp samples obtained at 150 °C for 20 h (Fig. 4C), the long-rod crystals were observed clearly, with the aspect ratio about 10 and the mean size around 15 × 150 nm. We also found that there are not too much differences in morphology and size from the photographs of HAp samples obtained at 120 °C for 12 h, 16 h, 20 h and 24 h. Generally, elongation of reaction time will result in crystal growth, but our experiment seems inconsistent with this. This could probably be attributed to the mediation of CTAB, as we will discuss in detail in the following paragraph. So we may conclude that, compared with the reaction time, the temperature of reaction plays a more important role in controlling the crystal morphology and size in this system.

As for the effect of CTAB, similar to other surfactant, it was thought to be able to act as a template [31], with the template action resulting in the epitaxial growth of the product. By the charge and stereochemistry

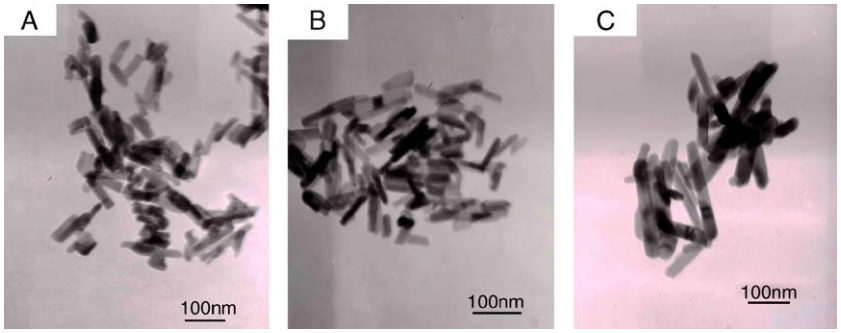

Fig. 4. The TEM photographs of HAp powders obtained at 120 °C for 20 h (A), 24 h (B) and at 150 °C for 20 h (C).

complementarity, a process called molecule recognition could have taken place at the inorganic/organic interface [16,17]. The added surfactant was supposed to bind to certain faces of crystal or to certain ions as well, so these ions could be incorporated to the existing nuclei at a steady rate and the final shape and size of HAp particles could be well controlled [32].

The behavior of CTAB in our work is also considered to correlate with the charge and stereochemistry properties. In an aqueous system, CTAB would ionize completely and result in a cation with tetrahedral structure. Meanwhile, the phosphate anion has also a tetrahedral structure. So the CTAB can be well incorporated to the phosphate anion by the charge and structure complementarity (Fig. 5). A probable mechanism for the templating process is that CTAB-PO_4^{3-} mixtures form rod-like micelles, which contain many PO_4^{3-} groups on the surface, and when Ca^{2+} is added into the solution, $Ca_9(PO_4)_6$ clusters [33] are preferentially formed on the rod-shaped micellar surface due to conformation compatibility between identical hexagonal shape of the micelles and $Ca_9(PO_4)_6$ clusters. The micelles act as nucleating points for the growth of HA crystals. During the hydrothermal stage, CTAB-HA complexes are produced and they coalesce to control the morphology and size of obtained HAp. Since the crystallization process is under critical control of CTAB, the resulting HAps were invariably nanorods with uniform morphology and controllable size.

4. Conclusion

Hydroxyapatite nanoparticles with uniform morphologies and controllable size have been synthesized by low-temperature hydrothermal method in the presence of cationic surfactant. The CTAB as a template is used to regulate the nucleation and crystal growth. The CTAB can bind with phosphate anion of reaction system by the charge and stereochemistry complementarity, so that phosphate anion can be incorporated to the existing nuclei at a steady rate and the final shape and size of HAp particles can be well controlled. Compared with the reaction time, the temperature of reaction is more significant variable in altering the HAp morphology and size.

Acknowledgments

The authors acknowledge the financial supports for this study from National Natural Science Foundation of China (NSFC) Project Grant (50272021, 59932050, and 50472054), Natural Science Foundation Cooperative Project Grant of Guangdong (04205786). We also thank Dr. B. Léon for her helpful comments and suggestions.

References

[1] K.D. Groot, Biomaterials 1 (1980) 47.
[2] J.D. Currey, The Mechanical Adaptations of Bones, Princeton University Press, 1984.
[3] L.L. Hench, J. Am. Ceram. Soc. 74 (1991) 1487–1510.
[4] K.D. Groot, Bioceramics of Calcium Phosphate, CRC PRESS, 1984.
[5] J. Torrent-Burgues, J. Torrent-Burgues, T. Boix, J. Fraile, R. Rodriguez-Clemente, Cryst. Res. Technol. 36 (2001) 1075–1082.
[6] J. Arensds, J. Chistoffersen, M.R. Chistoffersen, H. Eckert, J. Cryst. Growth 84 (1987) 515.
[7] G. de With, H.J.A. Van Dijk, N. Hattu, K. Prijs, J. Mater. Sci. 16 (1981) 1592.
[8] H. Aoki, Science and Medical Application of Hydroxyapatite, Japanese Association of Apatite Science, Tokyo, Japan, 1991.
[9] W. Suchanek, M. Yoshimura, J. Mater. Res. 13 (1998) 94.
[10] R.Z. Legeros, Calcium Phosphates in Oral Biology and Medicine, Karger, Basel, Switzerland, 1991.
[11] K. Wei, Y.J. Wang, C. Lai, C.Y. Ning, D.X. Wu, G. Wu, N.Y. Zhao, X.F. Chen, J.D. Jian, Mater. Lett. 59 (2005) 220–225.
[12] M. Yoshimura, H. Suda, K. Okamoto, K. Ioku, J. Mater. Sci. 29 (1994) 3299.
[13] A. Tiselius, S. Hjerten, O. Levin, Arch. Biochem. Biophys. 65 (1995) 132.
[14] B.R. Heywood, S. Mann, Adv. Mater. 4 (1992) 278.
[15] S. Mann, G.A. Ozin, Nature 382 (1996) 313.
[16] D. Walsh, J.L. Kingston, B.R. Heywood, S. Mann, J. Cryst. Growth 133 (1993) 1–12.
[17] D.H. Gray, S. Hu, E. Juang, D.L. Gin, Adv. Mater. 9 (1997) 731.
[18] H.B. Lu, C.L. Ma, H. Cui, L.F. Zhou, R.Z. Wang, F.Z. Cui, J. Cryst. Growth 155 (1995) 120.
[19] S. Mann, D.D. Archibald, J.M. Didymus, T. Douglass, B.R. Heywood, F.C. Meldrum, Science 261 (1993) 1286.
[20] S. Mann, Nature 365 (1993) 499.
[21] D.D. Archibald, S. Mann, Nature 364 (1993) 430.
[22] I. Weissbuch, F. Frolow, L. Addadi, M. Lahav, L. Leiserowitz, J. Am. Chem. Soc. 112 (1990) 7718.
[23] A. Firouzi, D. Kumar, L.M. Bull, T. Besier, P. Sieger, Q. Huo, Science 267 (1995) 1138.
[24] W. Suchanek, M. Yashima, M. Kakihana, M. Yoshimura, J. Am. Ceram. Soc. 80 (1997) 2805–2813.
[25] W.L. Suchanek, M. Yoshimura, J. Am. Ceram. Soc. 81 (1998) 765–767.
[26] B.O. Fowler, Structural Properties of Hydroxyapatites and Related Compound, Gaithersburg, 1968.
[27] S.J. Joris, C.H. Amberg, J. Phys. Chem. 75 (1971) 3172.
[28] J.B. Liu, X.Y. Ye, H. Wang, M.K. Zhu, B. Wang, H. Yan, Ceram. Int. 29 (2003) 629–633.
[29] K.C. Blakeslee, R.A. Condrate, J. Am. Ceram. Soc. 54 (1971) 559.
[30] Z.H. Cheng, A. Yasukawa, K. Kandori, T. Ishikawa, J. Chem. Soc., Faraday Trans. 94 (1998) 1501.
[31] F.C. Meldrum, N.A. Kotov, J.H. Fendler, J. Phys. Chem. 98 (1994) 4506.
[32] L. Yan, Y.D. Li, Z.X. Deng, J. Zhuang, X.M. Sun, Int. J. Inorg. Mater. 3 (2001) 633–637.
[33] K. Onuma, A. Ito, Chem. Mater. 10 (1998) 3346–6651.